SCATTERING OF ULTRASONIC WAVES BY DEFECTIVE ADHESIVE BONDS

Ricardo Leiderman, leider@mecanica.ufrj.br
Programa de Engenharia Mecanica, COPPE-UFRJ

Paul E. Barbone, **barbone@bu..edu**
Department of Aerospace and Mechanical Engineering, Boston University

Arthur M.B. Braga, abraga@mec.puc-rio.br
Departamento de Engenharia Mecanica, PUC-Rio

Abstract. *It is known that the global strength of multi-layered composite structures strongly depends on the quality of the adhesion between its constituent elements. Imperfections along adhesion interfaces can effectively compromise structure's performance. The characterization of such defects is a very difficult task. The main goal of this study is the development of an analytic-numerical method to simulate the acoustic field resulting from the interaction of ultrasonic waves and imperfect interfaces, helping in selection of parameters for ultra-sonic inspecting methods. In that sense the Quasi-static-approximation (QSA) is combined with the Perturbation method to allow modelling of interfacial non-uniform flaws. A recursive algorithm to evaluate displacements and generalized stress fields in composite layered plates, whose the adhesion interfaces are potentialy defective, is developed based on the invariant imbedding method. It is applicable to solve wave propagation problems in arbitrarily anisotropic layered plates and it is stable for high frequencies. An inspection simulation of a composite layered plate immersed in water is presented as illustration of the developed method application. Results of the simulation indicate the frequencies and angles of incidence where the scattering effect, which allow the characterization of non-uniform defects, is more significant.*

Keywords*: non-destructive evaluation, adhesive bond, interface of adhesion, scattering*

1. INTRODUCTION

This paper addresses the problem of ultrasonic inspection of adhesively bonded composites. The goal here is the development of a systematic modeling procedure which can be used to design ultrasonic inspection methods to detect adhesive flaws.

In any adhesive bond, there are two adherends, the adhesive layer itself, and the two interfaces between the adhesive layer and the adherends. In aerospace applications, adherend thickness are typically measured in millimeters, an adhesive layer has a typical thickness measuring hundreds of microns, while the interfacial layer associated with the interface of adhesion is just a few microns thick. By considering this interfacial layer to be infinitesimally thick, we can replace it by a set of equivalent springs. The springs connect the adhesive to the adherend, and enforce continuity of traction and (approximately) displacement. This approximation was apparently first proposed by Baik and Thompson (Baik and Thompson, 1984), who called it the quasi static approximation (QSA). In what follows, we use the QSA approximation to model the adhesive interface. Local imperfections in the adhesive interface are thus modeled by local changes in the spring stiffness representing the interface.

Several analytical approaches exist to model wave propagation in plane layered media. Of these, those that are based on propagator matrices are known to be numerically unstable at high frequencies. The major difficulty occurs when one or more wave type is evanescent. Variations of the method of invariant imbedding have been developed to overcome this difficulty (see for example Braga *et al.,* (1992) and (Wang and Rokhlin, 2002)). Here, we present a variation developed in Leiderman *et al*., (2005) to predict the sound scattered from a layered plate with adhesive flaws. The presented algorithm is equally well suited to treating anisotropic as isotropic layers and is both unconditionally stable and efficient. The method is suitable for modeling of the common ultrasonic inspection approaches. As such, it may serve to aid in the design of these methods, as well as a basis for inverse scattering. The former application is demonstrated here by identifying a rule for the optimal selection of scanning parameters, in this case, angle of incidence.

In the next section we begin our presentation with the problem formulation, and discuss the role of the quasi-static approximation for the adhesive interface. We then formally solve the problem by constructing a high order perturbation expansion of the exact solution. The perturbation parameter is the strength of the inhomogeneity in the adhesive layer. We then present the recursive invariant imbedding algorithm to solve for each term in the perturbation expansion. As an example, we apply the method to the case of a three-layered plate immersed in water. We show how to use our results to indicate the frequencies and angles of incidence at which the scattered field is most sensitive to localized interface defects.

2. PROBLEM FORMULATION

We consider a layered elastic structure submerged in an acoustic fluid. The solid consists of *N* layers, bonded together by adhesive bonds. We assume the *z-axis* is normal to the layering, and designate the plane *z=0* to be the ``bottom" of the plate, and *z>0* ``upwards", as indicated in Figures 1 and 2. In the fluid regions, $z< z_0 = 0$ and $z>z_N>0$, the fluid pressure satisfies:

$$\nabla^2 p + k^2 p = 0 \tag{1}$$

$$p = p_{up} + p_{down} \tag{2}$$

$$p_{up} = 0 \qquad z < 0 \tag{3}$$

$$p_{down} = p_{inc} = known \qquad z > z_N \tag{4}$$

In (2) we have decomposed the pressure field into up and downgoing components, respectively. The conditions (3) and (4) thus represent radiation conditions. In the equations above and in what follows, we assume and suppress a time dependence of $e^{-i\omega t}$.

The n^{th} layer of the solid is supposed to occupy $z_{n-1} < z < z_n$, and have elasticity tensor $\mathbf{C}^n$ and density ρ^n. Therefore, the stress $\boldsymbol{\sigma}$ and displacement $\mathbf{u}$ in the n^{th} layer satisfy:

$$\nabla \cdot \boldsymbol{\sigma} + \rho^n \omega^2 \mathbf{u} = 0 \qquad z_{n-1} < z < z_n \tag{5}$$

$$\boldsymbol{\sigma} = \mathbf{C}^n : \nabla \mathbf{u} \qquad z_{n-1} < z < z_n \tag{6}$$

We note that the n^{th} layer may be either a structural layer or an adhesive layer.

Making use of the quasi-static approximation (QSA) for the interface condition, as seen in Fig.1, gives us the following boundary condition at the interface between the n^{th} and $n+1^{th}$ layers:

$$\mathbf{K}[\mathbf{u}(z_n^+) - \mathbf{u}(z_n^-)] = \mathbf{t}(z_n^+) \tag{7}$$

$$\mathbf{t}(z_n^+) = \mathbf{t}(z_n^-) \tag{8}$$

Here, $\mathbf{K}$ is a diagonal spring matrix, $\mathbf{u}(z_n)$ is the displacement vector in the n^{th} layer, $\mathbf{t}(z_n)$ is the traction vector acting on the *xy* plane. We note that the entries in $\mathbf{K}$ are given in terms of the assumed thickness and elastic properties of the interfacial layer (Rokhlin and Huang, 1992). Higher order extensions of similar models for thin layers have recently been described in (Zakharov, 2006), (Wang and Rokhlin, 2004a) and (Wang and Rokhlin, 2004b).

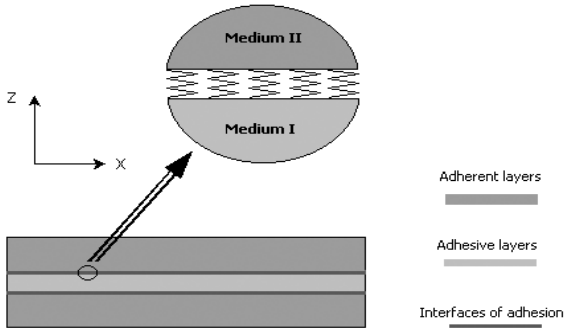

Figure 1. Quasi Static Approximation (QSA). When the inspecting wavelength to the interface-thickness ratio is large, interfaces of adhesion can be modeled as distributed transversal and normal springs.

Imperfections in the adhesive bond between layers may be modeled by a reduction in spring constants in $\mathbf{K}$. Since imperfections tend to be localized in space, this implies that $\mathbf{K}(x,y)$ must be allowed to depend upon position in the layer. Therefore, we write:

$$\mathbf{K} = \mathbf{K}_0 + \varepsilon \mathbf{K}_1(x,y) \tag{9}$$

Here, $\mathbf{K}_0$ is constant and $\mathbf{K}_1(x,y)$ is a function of the in plane position coordinates *(x,y)*. The dimensionless parameter ε represents the magnitude of the defect. A similar approach to represent localized defects can be found in Nakagawa et al., (2004). In the following, we determine the asymptotic expansion of the solution about the point $\varepsilon = 0$. In many cases of interest, the resulting series expansion converges. Accordingly, we expand the displacement and traction fields in the standard way:

$$\mathbf{u} = \mathbf{u}_0 + \varepsilon \mathbf{u}_1 + \varepsilon^2 \mathbf{u}_2 + \varepsilon^3 \mathbf{u}_3 + \ldots \tag{10}$$

$$\mathbf{t} = \mathbf{t}_0 + \varepsilon \mathbf{t}_1 + \varepsilon^2 \mathbf{t}_2 + \varepsilon^3 \mathbf{t}_3 + \ldots \tag{11}$$

Substituting (9-11) into the boundary conditions (7) and (8) leads to the following sequence of boundary conditions for each power of ε. For *O(1)* through *O(ε^2)*, we obtain:

$$\mathbf{K}_0[\mathbf{u}_0(z_n^+) - \mathbf{u}_0(z_n^-)] = \mathbf{t}_0(z_n^+) \tag{12}$$

$$\mathbf{t}_0(z_n^+) = \mathbf{t}_0(z_n^-) \tag{13}$$

$$\mathbf{K}_0[\mathbf{u}_1(z_n^+) - \mathbf{u}_1(z_n^-)] + \mathbf{K}_1[\mathbf{u}_0(z_n^+) - \mathbf{u}_0(z_n^-)] = \mathbf{t}_1(z_n^+) \tag{14}$$

$$\mathbf{t}_1(z_n^+) = \mathbf{t}_1(z_n^-) \tag{15}$$

$$\mathbf{K}_0[\mathbf{u}_2(z_n^+) - \mathbf{u}_2(z_n^-)] + \mathbf{K}_1[\mathbf{u}_1(z_n^+) - \mathbf{u}_1(z_n^-)] = \mathbf{t}_2(z_n^+) \tag{16}$$

$$\mathbf{t}_2(z_n^+) = \mathbf{t}_2(z_n^-) \tag{17}$$

and etc. The field equations in each layer (5) and (6) remain unchanged in form and are satisfied by each term in the series (10) and (11).

As seen in expressions (14) or (16), the terms $\mathbf{K}_1[\mathbf{u}_m(z_n^+) - \mathbf{u}_m(z_n^-)]$ can be understood as traction sources, or surface forces acting along the interface of adhesion. To simplify notation we will define φ_m for use in later sections of this paper:

$$\varphi_m^n = \mathbf{K}_1[\mathbf{u}_m(z_n^+) - \mathbf{u}_m(z_n^-)] \tag{18}$$

The equations above show that the *O(1)* terms satisfy the equations in a medium with no adhesion defects. This term will be called the specular field. Further, the terms of *O(ε^m)* are determined from the terms of *O(ε^{m-1})*. More precisely, the *O(ε^m)* terms satisfy the equations for a layer without defects, but with an acoustic source term determined from the defect and the *O(ε^{m-1})* field. Thus, in order to solve for each term in the series, we need consider the field radiated sources embedded in a plate without defects. The terms can be calculated in succession until the sum converges. We refer to the sum $\mathbf{u}_s^n = \varepsilon \mathbf{u}_1^n + \varepsilon^2 \mathbf{u}_2^n + \varepsilon^3 \mathbf{u}_3^n + \ldots$ as the scattered field.

3. RECURSIVE SOLUTION ALGORITHM

In this section we present a variant of the invariant imbedding method well suited to solve precisely the problem at each perturbation order. The presented algorithm is equally well suited to treating anisotropic as isotropic layers. A detailed derivation can be found in Leiderman *et al*. (2005).

We begin at the "bottom" of the plate ($z = 0$) where the plate is in contact with a known substrate. In the cases we consider, that substrate is a semi-infinite quiescent fluid, but extensions to other substrates are straightforward. At the surface of the known substrate, we know the acoustic impedance (for each $x-$ wavenumber) presented to the plate, and so can evaluate the boundary condition on the plate. The next step is to consider an elastic layer overlying an arbitrary substrate with known surface impedance and traction sources. The goal is to compute the surface impedance and traction sources acting on the top surface of the layer, in terms of the corresponding values on the bottom of the layer and the properties of the layer itself. After this, we perform a similar calculation with the elastic layer replaced by a "spring" interface which models the adhesion interface.

This gives us all the ingredients we need to solve the problem. We build these into a loop, in which the impedance and traction sources at each interface in the material are successively computed, starting at the bottom of the plate and ending at the top. Once the surface impedance and traction sources at the top are known, we impose the conditions of continuity of pressure and normal velocity at the top fluid interface. This formally completes the solution as both the incident and radiated pressures in the fluid above the plate are known. To evaluate the fields inside the plate, we must propagate the whole solution back down into the plate. We call this part of the solution the "backward sweep". The geometry of the problem tackled here is shown schematically in Fig 2.

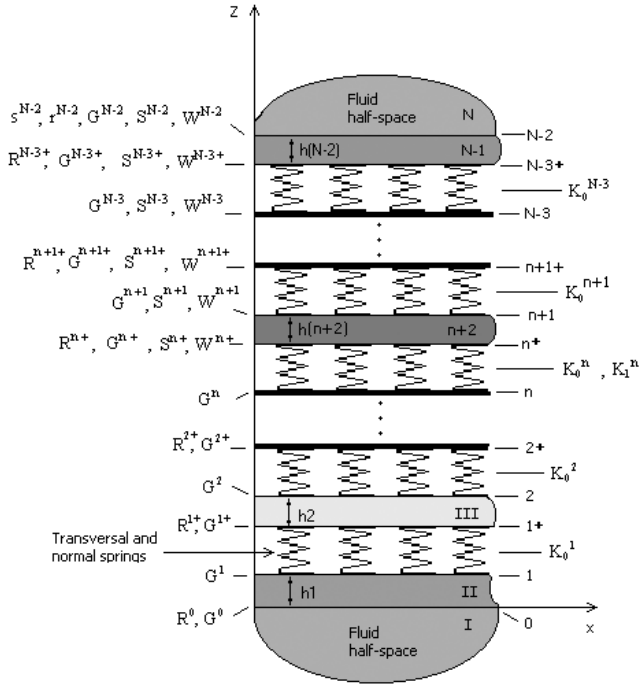

Figure 2. General problem consisting of a layered plate immersed in an acoustic fluid, in the context of the QSA. The layered plate is infinite in *x* and *y* directions and has its constituent layers joined by adhesive layers. *N* is the total number of layers plus two half-spaces and *n* stands for the *nth* layer or interface.

3.1. Elastic layer

Here we consider an elastic layer with thickness h resting on a substrate. The bottom of the layer is located at $z = z_0$. The top of the layer is $z = z_1 = z_0 + h$. The substrate upon which the layer rests has a known surface impedance $\mathbf{G}_o$ and traction source field $\mathbf{F}$. Thus, at $z = z_0$, in the substrate:

$$\bar{\mathbf{t}} = -i\omega \mathbf{G}_o \bar{\mathbf{u}} + \mathbf{F}_o , \tag{19}$$

where the bar over the field variables indicates a single Fourier transform over the coordinate *x*, indicating that we work in the *x*-wavenumber domain.

Our goal in this section is to evaluate the equivalent surface impedance and source field at the top surface of the elastic layer, while taking account of the substrate impedance and the elastic properties of the layer itself. In solving the equations of motion (5 & 6) in the elastic layer, we introduce “upgoing" and “downgoing" partial waves in the solid according to their wavenumbers in the vertical (z) direction. In particular, we denote by $\bar{\mathbf{u}}_1$ the sum of all upgoing (displacement) waves in the solid, and by $\bar{\mathbf{u}}_2$ the sum of all downgoing (displacement) waves in the solid.

The traction vectors (on planes of constant z) associated with each set of waves can be given in terms of the *local impedance tensors*, $\mathbf{Z}_1$ and $\mathbf{Z}_2$ as:

$$\bar{\mathbf{t}}_1(z) = -i\omega \mathbf{Z}_1 \bar{\mathbf{u}}_1(z) \tag{20}$$

$$\bar{\mathbf{t}}_2(z) = -i\omega \mathbf{Z}_2 \bar{\mathbf{u}}_2(z). \tag{21}$$

The impedance tensors $\mathbf{Z}_j$ are given in Leiderman *et al*. (2005).

At the bottom surface of the elastic layer, the boundary condition (19) applies. Thus:

$$-i\omega \mathbf{Z}_1 \bar{\mathbf{u}}_1(z_0) - i\omega \mathbf{Z}_2 \bar{\mathbf{u}}_2(z_0) = -i\omega \mathbf{G}_o[\bar{\mathbf{u}}_1(z_0) + \bar{\mathbf{u}}_2(z_0)] + \mathbf{F}_o. \tag{22}$$

Solving for $\bar{\mathbf{u}}_1$ gives us

$$\bar{\mathbf{u}}_1(z_0) = \mathbf{R}(z_0)\, \bar{\mathbf{u}}_2(z_0) + i[\omega \mathbf{Z}_1 - \omega \mathbf{G}_o]^{-1} \mathbf{F}_o \tag{23}$$

$$\mathbf{R}(z_0) = -[\mathbf{Z}_1 - \mathbf{G}_o]^{-1}[\mathbf{Z}_2 - \mathbf{G}_o] \tag{24}$$

The tensor $\mathbf{R}(z_0)$ introduced above is called the *reflection tensor* of the interface at $z = z_0$.

We now introduce two propagator matrices, $\mathbf{M}_1$ and $\mathbf{M}_2$:

$$\bar{\mathbf{u}}_1(z) = \mathbf{M}_1(z - z_1)\bar{\mathbf{u}}_1(z_1) \tag{25}$$

$$\bar{\mathbf{u}}_2(z) = \mathbf{M}_2(z - z_1)\bar{\mathbf{u}}_2(z_1) \tag{26}$$

Expressions for $\mathbf{M}_1$ and $\mathbf{M}_2$ are given in Leiderman *et al*., 2005. Thus, at the top of the layer:

$$\bar{\mathbf{u}}_1(z_1) = \mathbf{R}(z_1)\, \bar{\mathbf{u}}_2(z_1) + \mathbf{S}\mathbf{F}_o \tag{27}$$

$$\mathbf{R}(z_1) = \mathbf{M}_1(h)\mathbf{R}(z_0)\mathbf{M}_2(-h) \tag{28}$$

$$\mathbf{S} = i\mathbf{M}_1(h)[\omega \mathbf{Z}_1 - \omega \mathbf{G}_o]^{-1} \tag{29}$$

Here we introduced $\mathbf{S}$ which transports traction sources at $z = z_0$ into displacement sources at $z = z_1$. In (28) we took advantage of the fact that, due to its characteristics, the inverse of the matrix $\mathbf{M}_2(h)$ can be written as $\mathbf{M}_2(-h)$, avoiding eventual numerical troubles in the inversion.

The total displacement at the top of the layer can be given in terms of $\mathbf{u}_2$, the incident displacement field:

$$\bar{\mathbf{u}}(z_1) = [\mathbf{I} + \mathbf{R}(z_1)]\bar{\mathbf{u}}_2(z_1) + \mathbf{S}\,\mathbf{F}_o. \tag{30}$$

The total traction at the top of the layer, i.e. at $z = z_1$, can now be written in terms of $\bar{\mathbf{u}}$:

$$\bar{\mathbf{t}}(z_1) = -i\omega \mathbf{G}_1 \bar{\mathbf{u}}(z_1) + \mathbf{F}_1 \tag{31}$$

$$\mathbf{G}_1 = [\mathbf{Z}_2 + \mathbf{Z}_1\mathbf{R}(z_1)][\mathbf{I} + \mathbf{R}(z_1)]^{-1} \tag{32}$$

$$\mathbf{W} = [\mathbf{Z}_1 - \mathbf{G}_1]\mathbf{S} \tag{33}$$

$$\mathbf{F}_1 = -i\omega \mathbf{W}\, \mathbf{F}_o \tag{34}$$

Equation (31) is of the same form as the given boundary condition at the bottom of the layer, equation (19). These results show how the impedance of a layered elastic structure can be computed, layer by layer. The matrix $\mathbf{W}$ transports the effects of sources below a given elastic layer to the boundary condition at the top of the layer. The adhesion interfaces are modeled next.

3.2. Adhesion interfaces

The interface condition is:

$$\mathbf{K}_0[\bar{\mathbf{u}}(z_n^+) - \bar{\mathbf{u}}(z_n^-)] + \bar{\varphi}^n = \bar{\mathbf{t}}(z_n^+) = \bar{\mathbf{t}}(z_n^-). \tag{35}$$

Here as earlier, the superscript $+$ indicates the values of the field variables above the interface, while the superscript $-$ indicates those below. At the bottom of the interface, the adhesion interface is assumed to be in contact with an elastic layer, at the surface of which the following impedance boundary condition holds:

$$\bar{\mathbf{t}}(z_n^-) = -i\omega \mathbf{G}^- \bar{\mathbf{u}}(z_n^-) + \mathbf{F}^-. \tag{36}$$

To find the equivalent boundary condition at the top of the adhesive interface, we solve (35) for $u(z_n^-)$ and substitute into (36) to find:

$$\bar{\mathbf{t}}(z_n^+) = \bar{\mathbf{t}}(z_n^-) = -i\omega \mathbf{G}^+ \bar{\mathbf{u}}(z_n^+) + \mathbf{F}^+ \tag{37}$$

$$\mathbf{G}^+ = [\mathbf{I} + i\omega \mathbf{G}^- \mathbf{K}_0^{-1}]^{-1} \mathbf{G}^- \tag{38}$$

$$\mathbf{F}^+ = \mathbf{G}^- \mathbf{K}_0^{-1} \bar{\varphi}^n + [\mathbf{I} + i\omega \mathbf{G}^- \mathbf{K}_0^{-1}]^{-1} \mathbf{F}^- \tag{39}$$

3.3. Forward sweep

By using the results of this and the previous subsections, we can now determine the impedance of a layered plate with the lamina joined by adhesion interfaces modeled according to the QSA. The procedure is roughly as follows. We begin by considering a single elastic layer overlying a half-space. The half-space occupies the region $z < 0$ and has known impedance. We may now use (31) to determine $\mathbf{G}^1$ (see Figure 2), the total impedance at $z = h_1$, of the elastic layer/half-space system. Next we add a spring layer to the top of the elastic layer. We then compute $\mathbf{G}^{1+}$, the total impedance of the adhesion interface/elastic layer/half-space system by using (37). We continue to find the impedance of the system for each additional layer added to the system by alternately using equations (31) and (37). Eventually we compute $\mathbf{G}^N$, the total impedance of the entire laminated plate in contact with the upper half-space, and the corresponding transported source vector.

3.3.1.Getting started

To begin the forward sweep, we need the initial impedance values for a half-space. For an elastic half-space in which the radiation condition is satisfied at infinity, $\mathbf{G}^0 = \mathbf{Z}_2$. For a traction free surface at the bottom of the plate, we take $\mathbf{G}^0 = \mathbf{0}$. For a fluid half-space, a straightforward calculation gives the impedance as follows:

$$\mathbf{G}^0 = Z_f \mathbf{n} \otimes \mathbf{n} \tag{40}$$

$$Z_f = \frac{\rho_f \omega}{\beta} \tag{41}$$

In (40) we introduced $\mathbf{n}$, which represents the unit vector normal to the interface (i.e. in the $z-$direction.) The function $\beta = \beta(\omega, \alpha)$ is the wavenumber in the $z-$direction, which is computed from frequency ω and $x-$wavenumber α by $\beta = \sqrt{\omega^2/c_f^2 - \alpha^2}$. The sign is chosen in accord with the radiation condition; c_f denotes the sound speed in the fluid.

3.3.2. Scattering & radiation from top surface

Once we can compute $\mathbf{G}^N$ and $\mathbf{F}^N$, the impedance and transported acoustic sources at the top surface of the plate, we can formulate the reflection and radiation problem there. The boundary conditions in terms of the fluid pressure $\bar{\wp}$ and fluid normal displacement $\bar{w}_f$ at the top interface are:

$$\bar{\mathbf{t}}^N = -\bar{\wp}\,\mathbf{n} \tag{42}$$

$$\mathbf{n} \cdot \bar{\mathbf{u}}^N = \bar{w}_f . \tag{43}$$

These conditions enforce continuity of traction and normal displacement at the fluid/solid interface. Of course, we also have our impedance condition on the top surface of the solid:

$$\bar{\mathbf{t}}^N = -i\omega \mathbf{G}^N \bar{\mathbf{u}} + \mathbf{F}^N . \tag{44}$$

Substituting (42) into (44) and solving for $\bar{\mathbf{u}}$ gives

$$\bar{\mathbf{u}} = [i\omega \mathbf{G}^N]^{-1} (\bar{\wp}\,\mathbf{n} + \mathbf{F}^N). \tag{45}$$

As in every other layer, we decompose the pressure into downgoing (incident) and upgoing (radiated) fields,

$$\bar{\wp} = \bar{\wp}^{inc} + \bar{\wp}^{rad} . \tag{46}$$

Following steps analogous to those that lead to equations (23) and (24) leads us to

$$\bar{\wp}^{rad} = r\,\bar{\wp}^{inc} - \frac{Z_s Z_f}{Z_s + Z_f}\,\mathbf{n} \cdot [\mathbf{G}^N]^{-1} \mathbf{F}^N , \tag{47}$$

$$r = \frac{Z_s - Z_f}{Z_s + Z_f} , \tag{48}$$

$$Z_s = [\mathbf{n} \cdot [\mathbf{G}^N]^{-1} \cdot \mathbf{n}]^{-1} . \tag{49}$$

The right hand sides of (47-49) are all known. At this point, the solution at a given perturbation order is formally known.

In order to compute the solution at order $m+1$, we must know the interior displacement field at order m in order to evaluate the forcing terms in (18). We call that procedure the “backward sweep," and a full description can be found in Leiderman *et al.* (2005).

4. NUMERICAL SIMULATION

We present results of the simulation in this section. The example chosen corresponds to ultrasound inspection of a layered plate immersed in water. In particular, we show detection of a “kissing bond" in the plate. The plate is supposed to be composed of three layers: a copper layer with $3mm$ thickness, an epoxy layer with 200 μm thickness acting as the adhesive layer, and an aluminum layer with $3mm$ thickness. The plate is shown schematically in Fig. 3. It has, consequently, two internal adhesion interfaces: one between the copper and epoxy layers, interface b, and another between the epoxy and aluminum layers, interface a. The mechanical properties of its constituent materials are shown in Table I.

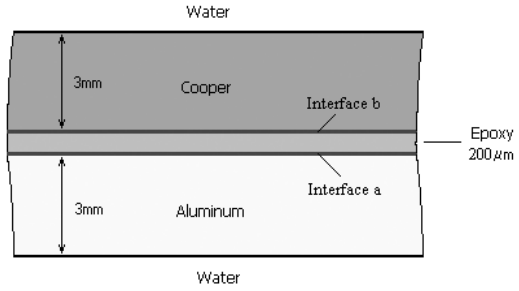

Figure 3. The modeled plate.

Table 1. Mechanical properties

Material	Density (Kg/m^3)	P-Wave speed (m/s)	S-Wave speed (m/s)
Aluminum	2700	6320	3130
Cooper	8930	4660	2660
Epoxy	1200	2150	1030
Water	1000	1480	0

The adhesion interface layers are assumed to have nominal thicknesses of 3μm each. When intact, they have the same mechanical properties as the epoxy. Accordingly, by the QSA model these interfaces can then be represented by the following spring stiffness matrix (Rokhlin and Huang, 1992):

$$\mathbf{K}_0 = \begin{bmatrix} 0.4259 & 0 & 0 \\ 0 & 0.4259 & 0 \\ 0 & 0 & 1.8457 \end{bmatrix} 1\times 10^{15}\ Pa/m \tag{50}$$

As mentioned above, the assumed bond defect models a “kissing bond." This is a region at the interface in which there is a strong contact between the two media, but poor adhesion. The contact allows the bond to transmit normal traction and displacement, without the ability to transmit shear traction or in-plane displacement. We modeled this defect by changing only the x component (i.e. the in-plane component) of the original adhesion interfacial stiffness. Thus, for interface *a* we assumed that the *xx* component of $\varepsilon \mathbf{K}_1$ is a Gaussian curve with maximum value equal to *90%* of the original interfacial stiffness, and its length approximately *5mm*, as shown in Fig. 4 - left.

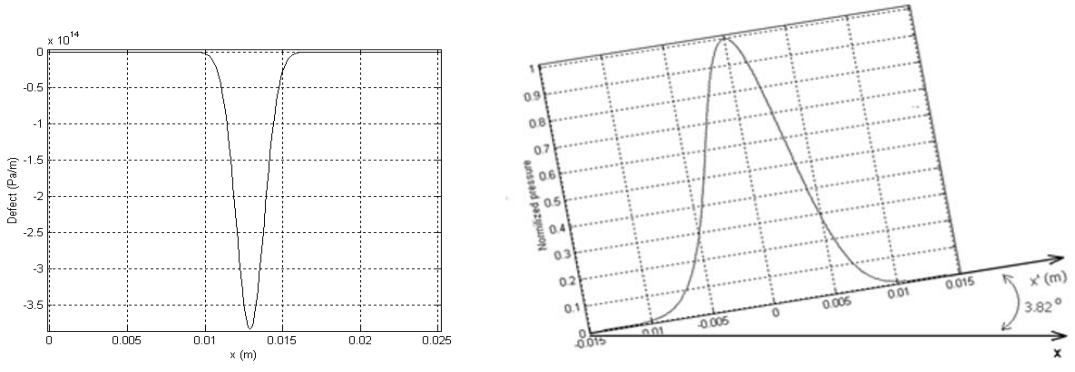

Figure 4. Left - The defect representing a *kissing bound*. Its maximum value is *90%* of the original stiffness of adhesion and its length is about *5mm*. Right - The acoustic incident field is a gaussian wave-beam with about 20mm of length and incident at the plate’s top surface with an angle of 3.82 degrees. The frequency is *4.9MHz*.

We chose the incident field to be an obliquely incident time-harmonic gaussian beam, with beam waist about *20mm* wide, frequency of *4.9MHz* and angle of incidence of *3,82*º. The frequency and angle of incidence were chosen to excite a leaky-Lamb mode in the plate that maximizes the scattered field (Leiderman *et al*., 2005). The incident field is represented schematically in Fig. 4 - right.

The spectra of the specular reflected and the scattered pressure fields in the upper fluid half-space are plotted in Fig. 5, left and right, respectively. Recall that by specular reflected field, we mean the field in the absence of a flaw, while scattered field is the difference between the total field and the specular field. It can be seen from these plots that the spectrum of the scattered field is much broader than the spectrum of the specular field, the latter having the same spectral width as the incident field. This broadening effect is associated with scattering of the incident signal by the defective interface. We also see, in the spectrum of the scattered field, significant amplitudes for negative propagation directions. These are associated with negative components of x-wavenumber, indicating pronounced back-scattering in the incident direction.

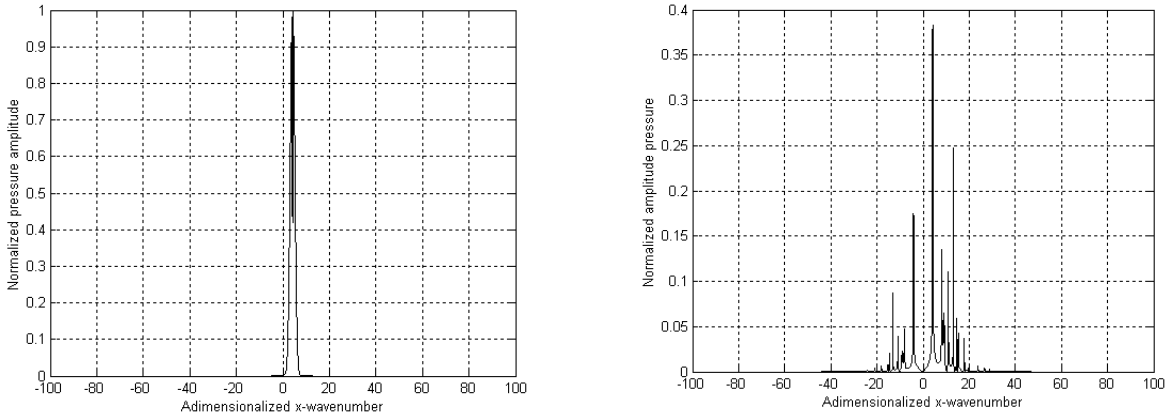

Figure 5. Left - Spectrum of the reflected pressure field. Right - Spectrum of the scattered pressure field.

The reflected acoustic energy fields are represented in Fig. 6. The plot at the left is related to the plate with non-defective interfaces, while the plot at the right is related to the plate with the kissing bond present in interface a. Data are plotted in dB for a better visualization of the difference between the two fields and the reference value is the maximum intensity of the incident field. The leaky-Lamb pattern is clearly shown at the left. Comparing the two figures shows the scattering effect resulting from the presence of the interface defect. For example, we see that the maximum intensity of the backscattered signal is about 30dB lower than the maximum intensity of the specular reflected field.

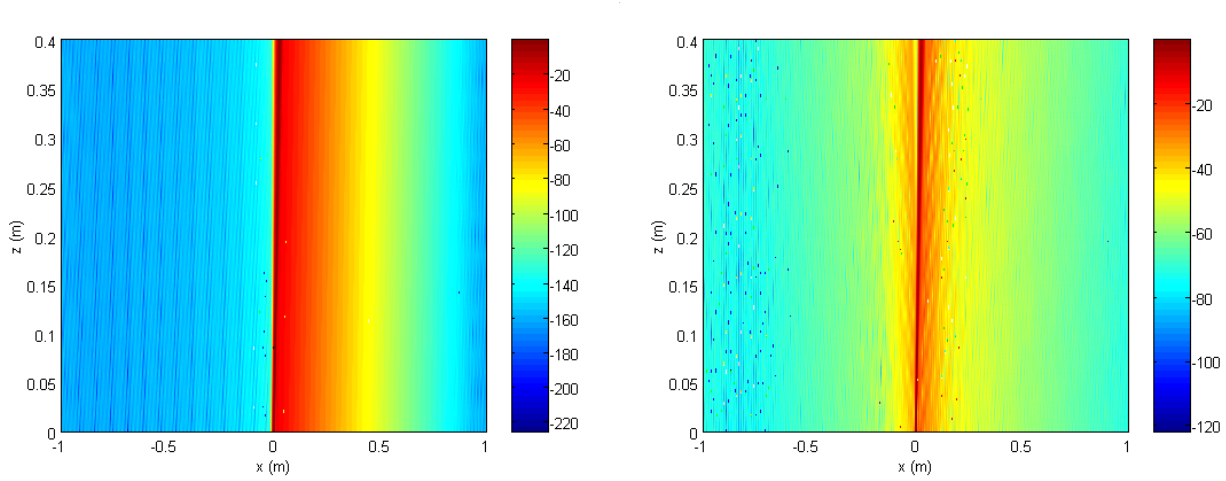

Figure 6. Left - The acoustic energy field related to the plate with homogeneous interface. Right - The acoustic energy field related to the plate with the defect present in the interface Data are plotted in Db where the reference value is the maximum value of the incident acoustic energy field.

5. SUMMARY AND CONCLUSIONS

We presented an analytic-numerical method to simulate the interaction of ultrasonic waves with imperfectly bonded plates. The primary ingredients in our solution are the QSA approximation for the adhesion interfaces, the perturbation method to account for non-uniform flaws, and the invariant imbedding method to give us numerical stability even for evanescent wave components at high frequencies. These combine to give us a recursive algorithm to evaluate displacements and generalized stress (pressure) fields in general problems consisting of composite layered plates. The algorithm is equally well suited to treating anisotropic as isotropic layers.

We illustrated the technique in Section 4 by simulating the ultrasonic inspection of an imperfectly bonded plate. These show that ultrasound can reveal the presence of kissing bonds. Such simulations can be used more generally in the design of ultrasound inspecting systems by exploring the design parameter space, such as frequency, angle of incidence, beam width, pulse length, etc. For pulse length, an additional Fourier transform is required.

6. ACKNOWLEDGMENTS

This work has been supported by the Brazilian Government through CAPES.

7. REFERENCES

Baik, J. M. and Thompson R. B., 1984, "Ultrasonic Scattering from Imperfect Interfaces: A Quasi-Static Model," *J. NDE,* Vol .14, pp177-196.

Honein, B.,, Braga, A.M.B., Barbone, P.E., and Herrmann, G., 1990, "Active suppression of sound reflected from a piezoelectric plate", *J. Intell. Mater. Syst. Struct.*, Vol. 3, pp. 209-223.

Leiderman, R., Braga, A.M.B., Barbone, P.E., 2005, "Scattering of ultrasonic waves by defective adhesion interfaces in submerged laminated plates", *J. Acoust. Soc. Am.*, Vol. 118(4), pp. 2154-2166.

Nakagawa, S., Nihei, K. T., and Myer, L. R., 2004, "Plane wave solution for elastic wave scattering by a heterogeneous fracture," *J. Acoust. Soc. Am.*, Vol.115, pp2761-2772.

Rokhlin, S. I. and Huang, W., 1992, "Ultrasonic Wave Interaction With a Thin Layer Between Two Anisotropic Solids," *J. Acoust. Soc. Am.*, Vol.92, pp1729-1742.

Wang, L., and Rokhlin, S. I., 2002, "A recursive stiffness matrix method for wave propagation in stratified media," *Boll. Seismol. Soc. Am.*, Vol.92, pp. 1129-1135.

Wang, L., and Rokhlin, S. I., 2004a, "Modeling of wave propagation in layered piezoelectric media by a recursive asymptotic method," *IEEE Trans.Ultrason. Ferroelectr. Freq. Control.*, Vol.51, pp. 1060-1071.

Wang, L., and Rokhlin, S. I., 2004b, "Recursive geometric integrators for wave propagation in a functionally-graded multilayered elastic medium," *J. Mech. Phys. Solids*, Vol.52, pp. 2473-2506.

Zakharov, D. D., 2006, "High order approximate low frequency theory of elastic anisotropic lining and coating," *J. Acoust. Soc. Am.*, Vol.119, pp1961-1970.

8. RESPONSIBILITY NOTICE

The authors are the only responsible for the printed material included in this paper.